Artificial Neural Networks Based Change Detection for Monitoring Palm Trees Plantation in Al Madinah-Saudi Arabia

Nermin A. Shoukry*

ABSTRACT

The selection of an appropriate change detection method is considerably significant in producing a high-quality change detection remotely sensed product. Many change detection techniques have been developed in a trial to achieve accurate results by using different remotely sensed data, different study areas, and different classification algorithms as a base for many change detection analysis techniques. Artificial Neural Networks (ANNs) is considered one of the most promising advanced artificial intelligence techniques to be applied in the classification analysis. This research generates a new approach for enhancing change detection analysis. It develops an advanced supervised ANNs-based change detection to detect temporal changes in palm trees plantation in the study area for two periods depicted in different multi-source, multi-temporal and multi-spectral satellite dataset. Preceding the classification analysis, a Median Spatial Convolution Filtering (MSCF) was applied for each temporal image. Additionally, a Normalized Difference Vegetation Index (NDVI) was used to transform multispectral data into a single gray scale image band representing vegetation distribution in each anniversary date image. The NDVI band was masked and infused into the ANNs classification procedures. Furthermore, This study adopts two main change detection algorithms, the *post-classification comparison* and the *change versus no-change binary mask*. Two change detection statistical matrix reports were produced, as well as two binary difference (decline or growth) maps for the two periods of study. Three assessments of accuracy were computed for the proposed ANNs method, as well as for the resultant binary difference maps. All overall accuracies exceeded 97% with Kappa coefficient above 0.96, providing a promising method for change detection enhancement analyses. **[Bul. Soc. Géog. d'Égypte, 2017, 90: 167-200]**

Key Words: Artificial Neural Networks, ANNs, Spatial Convolution, NDVI, Change Detection, Binary Difference Map, Accuracy Assessment.

1) Introduction and Literature Review

Different change detection algorithms have their own merits and no single approach is optimal and applicable to all cases (Lu *et al*., 2004). Processing of multi-temporal imagery and change detection approaches has been an active research field in remote sensing analyses for decades. In recent

* Department of Geography, Faculty of Arts, Cairo University, Giza, Egypt.

years, it was a challenging task for researchers to derive an accurate timely information on the earth's physical environment and human activities. It has been generally agreed that change detection is a complicated and integrated process. Therefore, the selection of an appropriate change detection method is considerably significant in producing a high-quality change detection product. The Artificial Neural Networks (ANNs) technique is considered one of the most complex and advanced algorithm that was recently and promisingly used in change detection analyses. It is a non-parametric supervised method that has the ability to estimate the properties of data based on the training samples.

It was not until the mid-1990s, however, that ANNs method was seriously recognized as an "artificial intelligent" approach and a promising classification algorithm in the remote sensing discipline. Numerous studies have demonstrated that neural networks can produce identical or improved classification accuracies to outcomes from conventional statistical classifiers (*e.g.*, Gopal & Woodcock, 1996; Serpico *et al.*, 1996; Mannan *et al.*, 1998; Ji, 2000; Zhang & Foody, 2001; Seto & Liu, 2003; Del Frate *et al*., 2007; Ashish *et al*., 2009; Pertopoulos *et al*., 2010; Deilmai *et al*., 2014; Ojaghi *et al*., 2015).

Mainly, the ANNs-based change detection technique has been used in such applications as forest mortality detection (Gopal & Woodcock, 1996; 1999), forest change (Woodcock *et al*., 2001), vegetation and land cover mapping (Fitzgerald & Lees, 1996; Foody *et al*., 1997; Foody, 1997), land degradation (Mann & Benwell, 1996), urban change (Liu & Lathrop, 2002), and integrating GIS data with images into applications of change detection (Deren Li, 2010).

During the past few years, researchers paid attention to the importance of studying some application cases concerning land use/ cover (LU/LC) change. The integration of artificial neural networks and remote sensing can help improve land cover mapping from remotely sensed data in a complex urban environment. Abuelgasim *et al*. (1999) introduced an adaptive fuzzy neural network classifier for environmental change detection to monitor land cover changes resulting from the Gulf war. This method succeed to predict land cover change with 86% accuracy. Dai & Khorram (1999) used a remotely sensed land cover change detection based on ANN by using multi-temporal landsat thematic mapper imagery with an overall accuracy of 95.6%. Zhou & Yang (2008) examined the use of ANN for land cover classification by applying Landsat ETM+ imagery on their study area. Their objective was to develop a guideline that would helps researchers for parameterizing the method. They tested 59 different parameters through trial and error method to come up with different accuracies. Ahmadizadeh *et al*. (2014) investigated in their paper the landuse changes using landsat TM images between 1986 and 2010. ANNs was used for classification and their overall accuracy was 89.67%.

In order to improve change detection accuracy and precision, different change detection techniques can be merged. More specifically, few studies have recently experienced the merging of ANNs supervised classification - as a single use algorithm or as a base of change detection analyses - with different techniques. Berberoglu *et al*. (2000) combined ANNs and texture analysis for land cover mapping. Liu & Lathrop (2002) applied Principal Component Analysis (PCA) to extract the salient features in their study area to reduce the dimensionality of the input data prior to the ANNs based change detection. Zhang *et al*. (2007) applied ANNs change detection to perform vegetation change detection. They combined the normalized difference vegetation index (NDVI) method with visual interpretation when identifying reference areas. Their procedure can reduce the topographic effect and improve the change detection accuracy. Mokhtarzade *et al*. (2008) extracted roads from high resolution IKONOS and Quick Bird satellite images and developed road detection technique by merging ANNs approach and co-occurrence texture analysis to produce road vectorization. They concluded that merging the two approaches gives a significant result.

2) Study Area and Data Source

2-1 Study Area

This study was carried out in the Islamic holy city of Al-Madinah Al-Munawarah - the urban capital city of Al-Madinah province - in the Kingdom of Saudi Arabia (K.S.A) (Figure 1). It is located in the north-western side of the kingdom to the east of the red sea between 39° 36’ 00” - 39° 42’ 36” East and 24° 21’ 00” - 24° 36’ 00” North. It covers an area of 560.101 square kilometers according to the city administrative boundary of the year of 2015. The study area has a unique site characterized by its multi-concentric irregular circular successive shape following mostly the multiple concentric city ring roads. Its geological and geographical structures are also unique. It is situated in a depositional basin surrounded by lava plateaus and hills within the western part of Arabian Shield, maintaining a variety of rich landscape types. The sub-soil in the city consists of nine soil types. The rocks vary from weak limestone to massive gabbro (Matsah & Hossain, 1993). It is surrounded by a number of mountains: Uhud to the north, Wa'rah to the north-east, E'yr to the south, A'zam to the west, and some other moderate heights hills. Moreover, it is situated on a flat mountainous plateau at the junction of some main valleys: Al-Aqoul, Al-Aqeeq, Al-Hamdh, Al-Nuqumi, and Batthan. Therefore, most areas of date palm tree farms are situated on the north, north-east, south, and south-east direction, including all recreational green spaces and public parks that are planted with date palm trees.

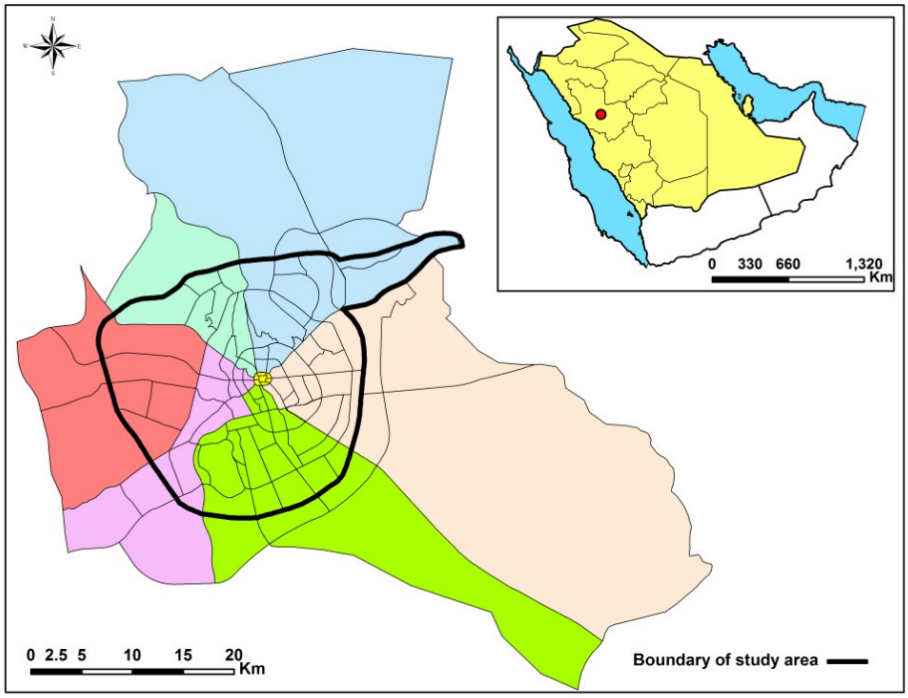

Figure 1. Location of study area.

2-2 Data Source and Acquisition

Three different multi-temporal and multi-spectral cloud-free satellite datasets were used for this analysis. All datasets were acquired from "King Abdulaziz City for Science and Technology (KACST)". The received satellite imagery has been geometrically corrected by the provider at the Universal Transverse Mercator (UTM) projection system, zone of 37N and at a World Geodetic Survey of the year 1984 (WGS-84) spheroid and datum. Although all datasets have the same satellite system "Landsat" that has the same temporal resolution and the same path and row (P/R=170/43), the three images have different remote sensor system differentiating between spectral channels' resolution, spatial resolution, and imagery radiometric resolution. All scenes were temporally selected carefully to have nearly same anniversary date for the research further analysis. The datasets cover a time period of 25 years. The first scene is a Landsat 5-Thematic Mapper (TM) image with acquisition date of September, 11, 1990. It has one emission spectral channel (band-6) with spatial resolution of 120 meters and six reflectance spectral channels (ranging from band-1 to band-7 except for band-6) with spatial resolution of 28.5 meters (resampled to 30 meters). Its radiometric resolution is 8 bits - values ranging from 0 to 255 raw digital number (DN) or brightness values (BV)

values -. The second scene is a Landsat 7-Enhanced Thematic Mapper Plus (ETM+) image with acquisition date of October, 13, 2005 with a radiometric resolution of 8 bits. It has one thermal infrared spectral channel (band-6) with spatial resolution of 60 meters, and one panchromatic reflectance spectral channel (band-8) with spatial resolution of 15 meters. The other six reflectance spectral channels have spatial resolution of 30 meters. The third scene is a Landsat 8- Operational Land Imager (OLI) image with acquisition date of September, 7, 2015 with a radiometric resolution of 15 bits (0-32767 DN values). It has two thermal infrared spectral channels (band-10 and band-11) with spatial resolution of 100 meters, and one panchromatic reflectance spectral channel (band-8) with spatial resolution of 15 meters. The other eight reflectance spectral channels have spatial resolution of 30 meters.

2-3 GIS Reference Vector Ancillary Data

A non-remote sensing data from a GIS can be used to assist in the analysis of remotely sensed images; such data form an ancillary or collateral data (Campbell, 1996). Representing the administrative boundary of the study area in 2015, a vector-GIS ancillary data in the form of a georeferenced shapefile was incorporated in the OLI 2015 satellite image to subset all the other imagery datasets based on the selected administrative boundary.

3) Basic Concepts of the Research Analyses

3-1 Spatial Convolution Filtering

A linear spatial filter is a filter for which the brightness value ($BV_{i,j}$) at location *i, j* in the output image is a function of some weighted average of brightness values in a particular spatial pattern around the *i, j* location in the input image. This process of evaluating the weighted neighboring pixel values is called two-dimensional *convolution filtering* (Jensen, 2005). The use of this procedure is usually used to eliminate random noise. A *median spatial convolution filtering* (MSCF) is proved to be a good process for removing "salt and pepper" noise or speckle from the image. The usage of this filtering process prior to the classification process smoothens the image, while preserving edges larger than the kernel dimensions. The median filter works by replacing each central pixel with the median value within the neighborhood specified by the filter kernel size window.

3-2 Normalized Difference Vegetation Index (NDVI)

Vegetation indices are quantitative measures based on digital values that attempts to measure biomass or vegetative vigor (Campbell, 1996). It have been developed for the enhancement of spectral differences on the basis of strong vegetation absorbance in the red and strong reflectance in the near

infrared part of the spectrum. One of the first successful vegetation indexes based on band rationing was developed by Rouse *et al*. (1974). They computed the normalized difference of brightness values (BV) from two satellite images for monitoring vegetation. They called it the *normalized difference vegetation index*, hereafter referred to as NDVI. The basic idea of this method is to compare reflectivity of the near infrared (NIR) - [NIR: is useful for crop identification and emphasizes soil-crop contrast] - and red (R) - [R: is called the chlorophyll absorption band that monitors healthy green vegetation and emphasizes vegetation discrimination] - reflectance spectral channels of the satellite image. Furthermore, it is an indicator, which numerically determines the amount of green vegetation. Thus, it is also referred as the greenness index. Therefore, the ratio of the amounts of reflectance in the (NIR) and (R) wavelength bands is computed using the equation: NDVI = (NIR - R) / (NIR + R).

3-3 Artificial Neural Networks (ANNs)

The area of ANNs is one of the sophisticated techniques in the area of artificial intelligence (AI) - sometimes called computational intelligence (CI) - known as nature inspired. The first wave of interest in neural networks (also known as "connectionist models" or "parallel distributed processing") was emerged in the field of Neuropsychiatry of Medicine science after the publishing of the scientific paper that experimented the nervous activity by McCulloch and Pitts in 1943 (McCulloch & Pitts, 1943). They developed simplified neurons in order to study the characteristics of human nervous activity and behavior by implementing theoretical neurophysiology to mathematical biophysics. In 1958, Rosenblatt proposed the theorem of the perceptron model as a mechanism of supervised learning (Rosenblatt, 1958). The perceptron consists of a single neuron which is considered later as the simplest form of a single neuron. Moreover, Minsky and Parpert published their book *Perceptron* in 1969 after several unsuccessful attempts from other researchers (Minsky & Parpert, 1969). In their book they showed the deficiencies of perceptron models. In that time, only few researchers continued their effort in this field. The interest in neural networks re-emerged and renovated by researchers in many scientific fields especially in the geo-computational analyses in remote sensing science in the early and mid-nineties as it is mentioned above.

Essentially, ANNs replicates - on a very limited scale - the behavior and connectivity among biological neurons in a brain. Briefly, the biological neuron is a cell that is stimulated by electrical impulses from other cells to which it is connected. If the cell receives enough stimuli, it sends out its own impulse (Keiner, 1999). Therefore, ANNs analysis can be operate as a complex mathematical function that converts input data such as "a remotely

sensed imagery" to a desired output such as "a land cover classification". In the supervised classification analysis, this function is usually accomplished by determining a set of training sites or samples. During the training phase, ANNs establish association between input and output data by establishment of weights within one or more hidden layers. Once trained based on the parameterization process, the ANNs can recognize unseen objects as it has the ability to generalize the output classes just as well.

There are two main types of ANNs topology - called architectures - exist, *feed-forward* and *feed-back* networks. The feed-forward architecture is more commonly applied for classification, clustering, function approximation and forecasting. The feed-back network is more complex - contains loops that may perform many repetition in the calculations - and more commonly applied for solving complex optimization problems (Peterson and SÖderberg, 1993). In the ANNs' feed-forward architecture (Figure 2), the flow of information occurs from the input layer to the hidden layer(s) and then to the output layer with no cycles or loops. There are several methods that were used to minimize the error between the network's output and the desired output in the classification analysis. The Back-propagation (BP) method (sometimes referred to as "backprop.") is the most commonly used method for ANNs classification. This method involves processing a set of input data and comparing the ANNs prediction to the corresponding outcome in the database. Therefore, it is the best method to be used for finding the optimal weights. Similar to the neighborhood search process in the conventional analysis, this study implements a multi-layered artificial neural networks' feed-forward technique with standard back-propagation algorithm for supervised analysis.

The ANNs architecture consists of a large number of processing units and a set of parameters that allow the researchers to parameterize the method according to their objectives. It can be defined as follows:

- A set of processing units called neurons, or nodes, or cells. Each neuron refers to only one input training class.
- Hidden layers (HL) that are determined by the user during the Neural Networks parameterization. A small number of HL should be determined if the training sample size is small or moderate as well as the number of classes. Using a large number of HL for great number of classes or large sample size will increase the computational complexity of the analysis
- Weighted connections that link neurons together according to specified activation function.

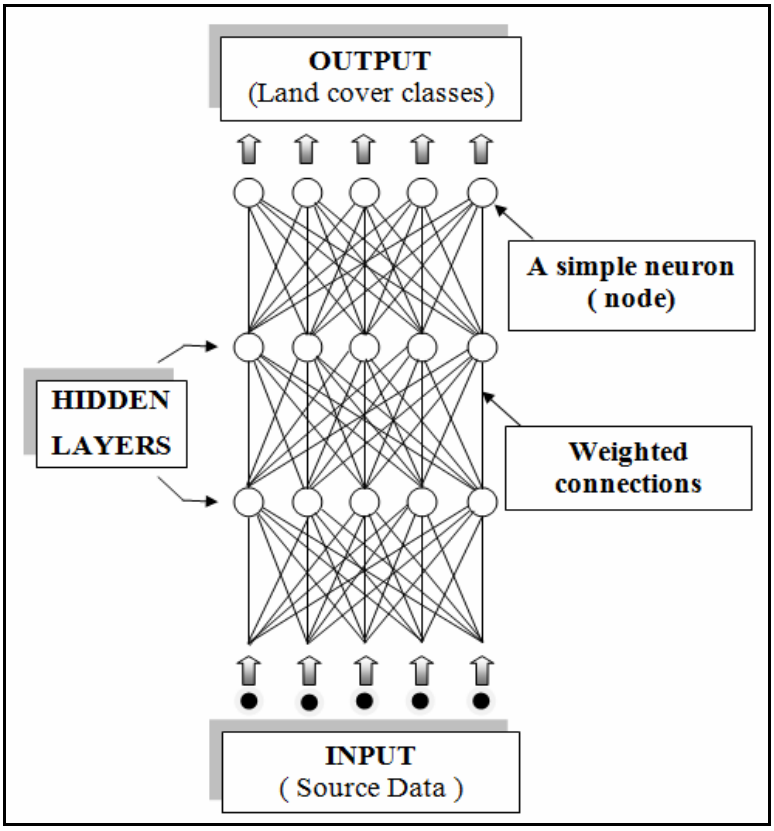

Figure 2. The ANNs "feed-forward network" architecture.

- Activation function (AF) that gives the network its ability to model non-linear behavior. There are two non-linear activation functions: the logistic (sigmoid) and the hyperbolic tangent. The logistic AF is the most widely used function that produces the output signal over zero to (+1) closed range, while the hyperbolic AF produces the scaled output over the (-1) to (+1) closed range.
- Training threshold contribution (T-Th) that determines the size of the contribution of the internal weight with respect to the activation level of the neuron. Its value should range from zero to one. Experiments on identifying the best threshold value stated that the closer to the value of one the finer the classification.
- Training Rate (TR) that specifies the magnitude of the adjustment of the weights.
- Training Momentum (MO) that controls the speed and effectiveness of the process depending on TR specified parameter.

- Training Root Mean Square Errors (T-RMS_E) exit criteria that determines the stopping criterion for the training processing.
- Number of Training Iterations (Iter.No) that determines the number of processing performance time.

3-4 Change Detection Analysis

Simply, change detection analysis can be identified as the use of multi-temporal datasets to discriminate areas of land cover change between two dates of imaging (Lillesand & Keifer, 2000). Rapid changing of physical and human geographical features and their frequent dynamism over time requires performing regular inventory on such changes. This will allow researchers and decision makers to understand and easily analyze both physical and human processes. Therefore, the most useful information that can be extracted from satellite imagery for this analysis is the "from-to" information that can be demonstrated in the form of maps and statistical matrices that are produced in tabular form. Change detection analysis embodies a wide range of methods or algorithms that monitor and quantify differences between two images of the same area with two dates difference; one is in an initial (former) state and the other is in the final (later) state. This study adopts two main change detection algorithms, the *post-classification comparison* and the *change versus no-change binary mask*.

The *post-classification comparison algorithm* is considered as the most accurate and commonly used approach in the change detection analysis. It provides "from-to" change class information. In addition, it requires rectification, resampling (if necessary), and classification for both two-date images independently. Then, when running the algorithm, the two classified images were compared on a pixel-by-pixel basis to determine those pixels with "a change" between land cover classes in the two dates. This method produces both statistically and spatially final results. The change detection statistics result is compiled in the form of a matrix to express the specific nature of the changes for each land cover class between the dates of imagery. The spatial result is produced in the form of a change detection map.

The *change versus no-change binary mask* is another efficient approach to delineate change in multi-date classified imagery. The change here is delineated to compare only the specified "similar" land cover class(es) from the resultant two-date classified image. This approach begins with classifying the two-date images. After running the classifier algorithm to generate a classified image, a masking process of the image spectral bands is performed to create a binary mask band (zero or one values) for each class individually in each year. Then a compute difference map algorithm is processed to subtract the former (initial) binary mask image from later (final)

binary image. A spatial resultant single-band growth image is produced for the time period of study (Shoukry, 2004).

Prior performing the change detection analysis, several remote sensing system conditions and environmental considerations must be accomplished by the analyst to obtain higher accuracies and give a significant impact on the success of the analysis. These conditions are as follows:

1. ***Temporal Resolution*:** Ideally, change detection analysis should be processed by using satellite imagery data sets that are acquired by the same satellite system, same satellite scanning system, same instantaneous field of view (IFOV), and same sensor system that acquires remotely sensed data at nearly exact same time of day for the multi-date images. In one hand, it is almost impossible to fulfill all of these conditions together, but on the other hand, it is mandatory to choose some of them. Often, *anniversary dates* are required in such analysis (for example, September, 7, 1990 & September, 7, 2015). But due to the difficulty of obtaining multi-date satellite images that have the exact same anniversary dates, a time difference of one month apart (before or after) in the same season is acceptable and it is called then a "near-anniversary dates images". It is proved that using anniversary date imagery minimizes sun angle and plant seasonal differences.
2. ***Spectral Resolution*:** Precautions must be taken by analysts to select the exact wavelength intervals in the electromagnetic spectrum (bandwidth) that a sensor can record in the two-date images. Unfortunately, different sensor systems do not record energy in exactly the same portions of bandwidths. Ideally, the same sensor system is used to acquire imagery on multiple dates. When this is not possible, the analyst should select bands that approximate one another - for example, Landsat 5 - TM bands (B): 2 (green), 3 (red), and 4 (near-infrared) can be used and match successfully with Landsat 8 - OLI bands: 3 (green), 4 (red), and 5 (near-infrared).
3. ***Spatial Resolution*:** Having the same pixel size in the multi-temporal satellite datasets is essential to successfully accomplish the analysis. If the multi-date imagery consist of different pixel size among them, a resampling process is required. Identifying this uniform pixel size is specified based on the analyst decision who should select a base image as a reference. Following the resampling process, a geometric rectification algorithm must be applied considering unifying the map projection and datum for all datasets. Rectification should be generated in all images by measuring a total "Root Mean Square Error (RMS_E)" of ≤ 0.5 pixel.
4. ***Radiometric Resolution*:** It refers to the dynamic range. If radiometric resolution differentiates between the multi-date datasets, a conversion process should be applied. For example in this study, when comparing 8-

bits image [having brightness values (BVs) ranging from zero to 255] with 15-bits image [having BVs ranging from zero to 32767], a mathematical process should be applied to have the same radiometric precision for all images.

5. ***Storage Data Formats (S.F)*:** Different multi-dates imagery datasets should have same storage format. There are three main S.F as follows: BIL (band interleaved by line), BSQ (band sequential), and BIP (band interleaved by pixel). If the datasets have different S.F in one date, a conversion processing should be applied.
6. ***Classification Analysis*:** Same classification analysis (supervised versus unsupervised) must be chosen for all multi-date images.
7. ***Classification Decision Rule (method or algorithm)*:** Same classification method is required to be processed for all multi-date imagery.
8. ***Land cover classification classes*:** In case of supervised classification, the analyst should design the same land cover classification scheme for all multi-date imagery. As for the unsupervised classification, the analyst should identify, adjust, merge, and rename the land cover classes to be the same for all date images.
9. ***Parameterization*:** Same sets of parameters must be chosen prior to the processing procedure for all multi-date imagery.
10. ***Image spatial dimension (Dims.)*:** Same image spatial dimension for former and later image is required.
11. ***Other environmental considerations*:** Jensen in 2005, specifies four environmental conditions that should be investigated to conduct the change detection analysis for the multi-date satellite images. These considerations are: firstly, the atmospheric conditions that specify that all images should be with no clouds, stratus, or extreme humidity on the days remote sensing data are collected. Secondly, the soil moisture condition should be identical for the multiple dates of imagery used in the analysis. Thirdly, considering vegetation phenology and lastly, considering the effects of tidal stage on image classification especially for coastal change detection analysis.

3-5 Measurement of Accuracy Assessments

Accuracy defines "correctness", it measures the agreement between a standard assumed to correct and a classified image of unknown quality. if the classified image corresponds closely with the standard, it is said to be accurate (Campbell, 1996). The assessment of the accuracy of computer-generated map derived from remote sensing data is fraught with difficulties, both practical and theoretical. On the practical side, there is the problem of selecting a reliable verification data, such as large topographic maps or a set of aerial photographs. On the theoretical side, the question of the appropriate mathematical or statistical procedure to establish estimates of accuracy

arises. In addition to these considerations, the issue of cost and efforts is that it always appears in any real-world remote sensing field verification.

This research generates two accuracy assessment procedures. The first is developed for the ANNs resultant classified images of all classes. While the second is for evaluating the accuracy of the resultant binary "palm trees plantation" difference (growth or decline) images of the two periods of study. To accomplish this goal, the study represents a classification error matrix, that is a method - also called the *confusion matrix* or *contingency table* - of characterizing the performance of the proposed classification technique. It is a standard form for reporting site-specific error. The matrix statistically computes and compiles errors and accuracies. There are two types of errors, such as omission errors (OE) and commission errors (CE). In addition to these errors, four types of accuracies are computed, such as the consumer's accuracy (CA), the producer's accuracy (PA) - also called "user's accuracy" -, the overall accuracy (OA), and the Kappa coefficient (κ or κ_{hat}) .

The errors of omission (also called errors of exclusion) represent the percentage of pixels left out of class. These pixels belong to the ground truth class but the classification technique has failed to classify them into the proper class. The errors of commission (also called errors of inclusion) represent the percentage of extra pixels in a class. These pixels belong to another class that are labeled as belonging to the class of interest. Producer and user accuracies are calculated as well in the error matrix. The producer accuracy is a measure that indicates the percentage of actual reference test pixels that were properly classified and are related to omission errors, while the user accuracy is a measure that indicates the percentage of classified pixels and actually represents that category on the ground and is related to commission errors. Moreover, an overall accuracy is computed by dividing the total number of correctly classified (sum of the major diagonal) by the total number of pixels in the error matrix (total sample size) (Jensen, 2005) for each image. The overall accuracy only incorporates the major diagonal and excludes the omission and commission errors. The Kappa coefficient express the proportionate reduction in error that was generated in the classification process, compared with the error of a completely random classification.

4) Research Methodology

Figure (3) is a flow chart of the proposed technical approach used in this research. The proposed technique involves integrating several techniques such as spatial convolution filtering, NDVI, ANNs, and change detection. The analysis was conducted by using the commercial remote sensing software ENVI® "Environment for Visualizing Images".

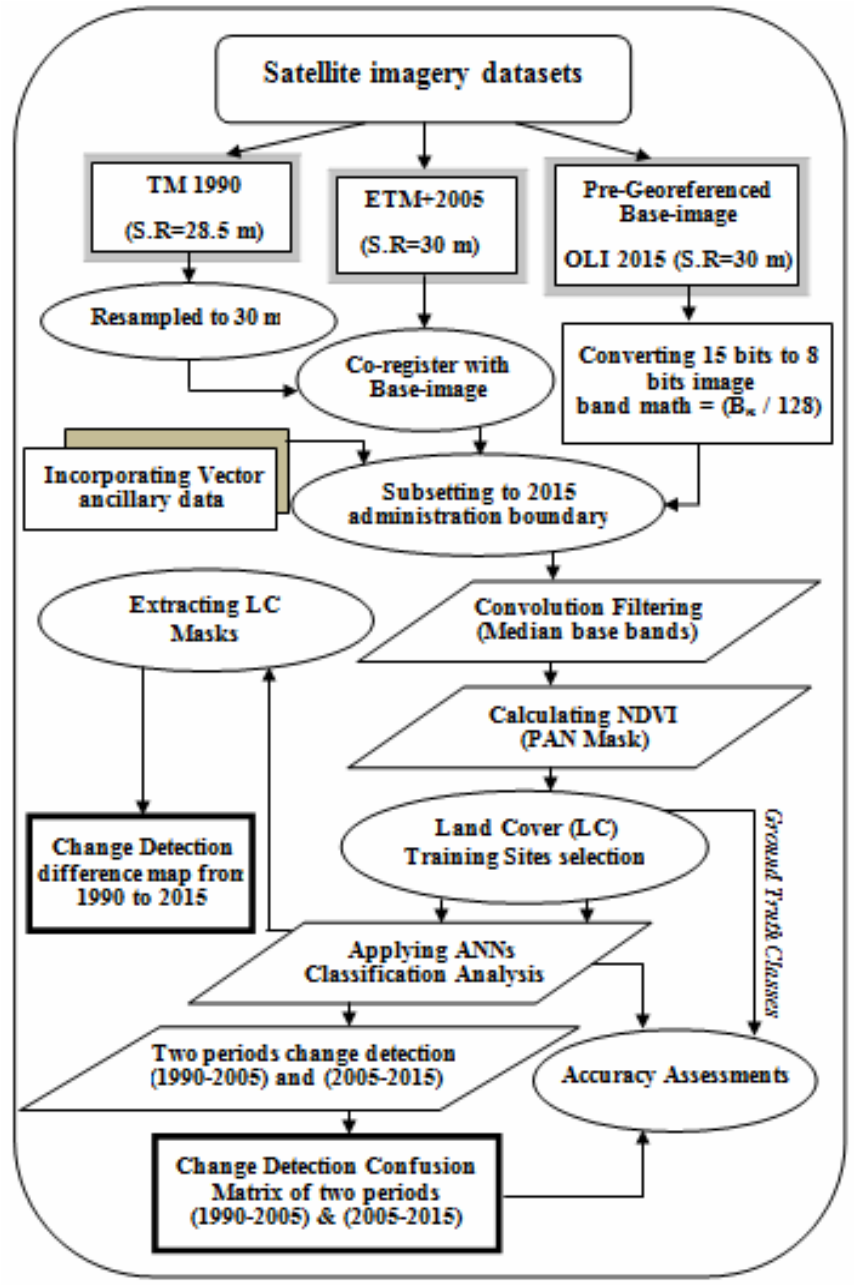

Figure 3. Flowchart of the proposed ANNs-based change detection method.

4-1 Data Preparation and Pre-processing

Dealing with multi-temporal image datasets requires that images obtained by sensors at different dates are comparable in terms of geometric and radiometric characteristics. This usually does not happen even for images generated by the same sensor. Precise registration of the satellite imagery datasets to ground coordinates was considered vital to this research. After obtaining the pre-georeferenced three-date scenes of the study area, the data preparation procedures begin with selecting a reference or a base-image. The OLI-2015 is selected as a base-image. Yet, this selected image has different and higher radiometric resolution (15 bits BVs) than the other two images (each has 8 bits BVs). In this case, it is preferable to convert higher radiometric resolution to lower-resolution data. Therefore, a conversion procedure using simple mathematical equation is generated for all the image' spectral bands. The equation of [$band\text{-}BV_n / (2)^7$] is processed by using the "band-math" subroutine in ENVI software to preserve the BVs values and to maintain same brightness effects of each pixel without losing data. Geometric correction has been verified for the OLI-2015 image as well as the vector-GIS ancillary data. The incorporated vector-GIS data was previously digitized to the updated administrative boundary of the study area in 2015, and geometrically rectified at (UTM) projection system and a (WGS-84) spheroid and datum. In a parallel procedure, the TM-1990 satellite image was resampled up from its 28.5 meters to a 30 meters pixel size in order to fulfill the change detection condition of matching spatial resolutions of all multi-temporal images.

In order to achieve the highest possible accuracy to eliminate or minimize as possible the spatial shifting between the three dates images, a second co-registration process should be employed to refer the other two (1990 & 2005) images to the reference image. The co-registration process is accomplished with a first order polynomial linear transformation and with a nearest neighbor resampling method. The Root-Mean-Square errors (RMS_E) for both image were < 0.2 pixel.

Based on the vector-GIS data incorporation, a dimension of (1197 × 937 Dims) was extracted and subsetted for all datasets from the whole scene to cover the study area with its 2015 administrative boundary (Figure 4). The false color composite of the three-date images is different from one another due to its bands' disorder. The reason for this differentiation is the different satellite sensor system of each image in this study.

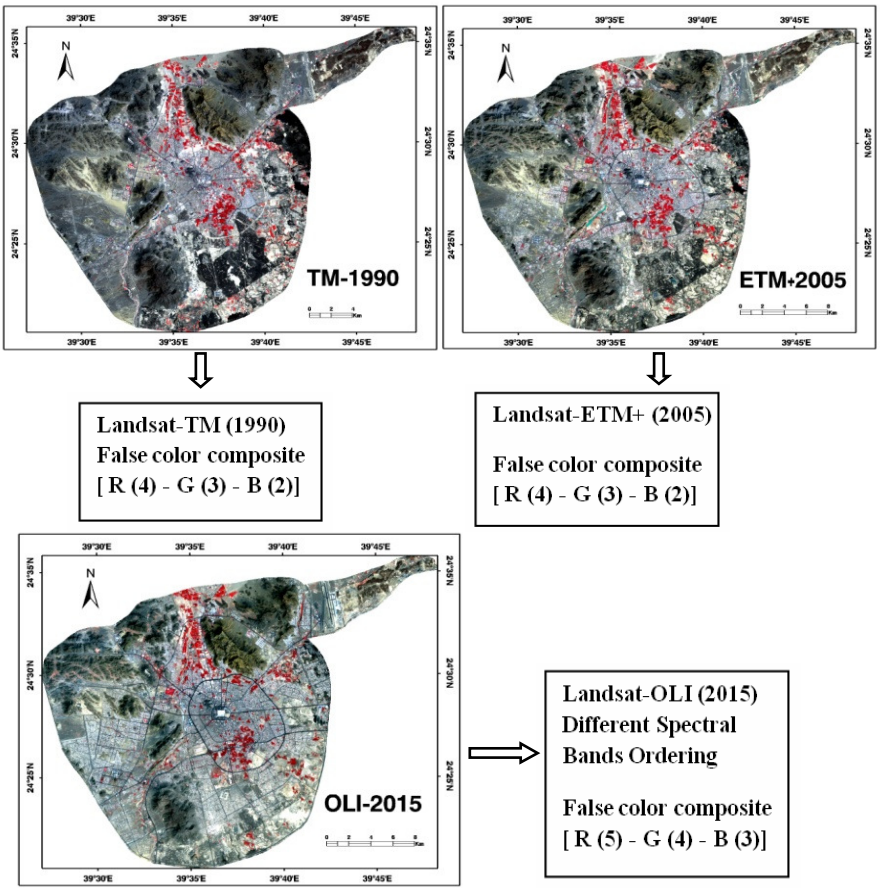

Figure 4. Different false color composites of the satellite imagery datasets.

4-2 Spatial Convolution Filtering & NDVI Masking

Since the main goal of this research is to achieve an accurate change detection analysis on the base of an artificial intelligent classification, two other methods should be integrated to the analysis. These methods are the spatial convolution filtering and the NDVI masking. Integrating all of these methods together would create a composite analysis with fine accuracy and result. To accomplish the integration process, certain data preparation should be ensured.

A two dimensional median spatial convolution filtering is applied for all reflective bands in all multi-spectral and multi-date images of the study area. A (3 × 3) kernel size window was applied to filtering process. The resultant multi-spectral bands images would be used in a later process as

bases for the classification analysis. Afterwards, NDVIs transformation were applied to the imagery datasets (Figure 5). Due to the disordering of the images' spectral bands, selection for the red and the NIR band is differentiated. As for the landsat-TM (1990) and the landsat-ETM+ (2005) images, band-3 (Red) and band-4 (NIR) were substituted in the NDVI equation. While the landsat-OLI (2015) used band-4 (Red) and band-5 (NIR) in the NDVI equation. The resultant mono-spectral band for each year would be infused as an additional mask band into the classification process.

4-3 Classification Scheme and Training Sites

A priori supervised classification approach was used to design the land cover classification scheme and to identify the training sites. The designed land cover (LC) classification scheme was determined based on a text annotated print out map of merged IRIS-Landsat satellite images and detailed topographic map (both with map scale of 1:50,000) that were published by the General Directorate of Military Survey of K.S.A (GDMS, 2001). Another precautious trial was accomplished before designing the LC scheme. This trial was an attempt to maintain precision of the selection of land cover classes and to try to eliminate or reduce as possible the gap between spectral & informational classes. Therefore, a trial of applying an ISODATA-unsupervised classification was achieved to identify the spectral classes of the study area. Based on the above considerations, four major land cover classes were designed as follows: (1) vegetated area, (2) urban/built-up areas, (3) bare land/soil, and (4) mountainous area. Based on the designed LC scheme, 11 informational classes were selected as training sites. Table 1 shows the classification scheme design and the training sites with their pixels' number for the three-dates satellite imagery of the study area.

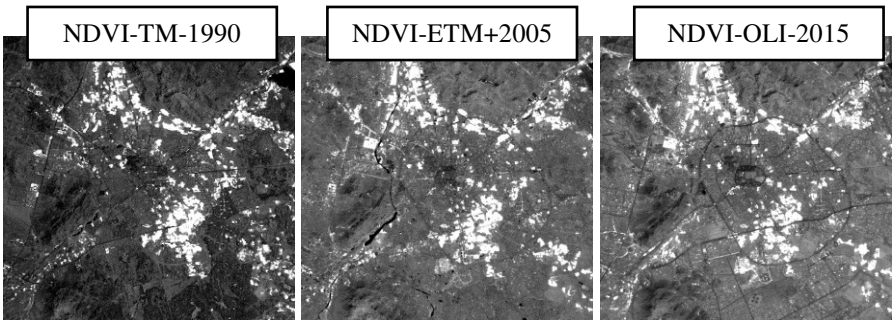

Figure 5. Subsets of NDVI mono-spectral bands derived from the satellite imagery datasets (white pixels represent palm plantations/public parks).

Table 1. Designed LC classification scheme and training sites selection.

Land Cover Classes	Number of pixels		
	TM-1990	ETM+2005	OLI-2015
(1) Vegetated Area			
(1.1) Palm Trees Plantation	1,600	1,528	1,349
(2) Urban/Built-up Areas			
(2.1) Roads/Asphalt	1,136	1,002	1,205
(2.2) Built-up Areas	996	1,073	1,016
(2.3) The Haram	22	106	305
(3) Bare Land/Soil			
(3.1) Bare-Sandy Land	1,473	1,526	1,576
(3.2) Red Soil	124	175	N/A
(4) Mountainous Area			
(4.1) Mountainous Area-1	1,018	1,432	1,303
(4.2) Mountainous Area-2	1,491	774	403
(4.3) Volcanic Lava Remains-1	1,325	1,040	904
(4.4) Volcanic Lava Remains-2	1,317	1,034	746
Outside Area	**57,498**	**94,018**	**26,985**

4-4 Artificial Neural Networks Classification Procedures

As was mentioned above, the resultant MSCF of the three-date images were used as bases for the classification analyses with the inclusion of the NDVI mask band for each dataset.

Setting the rightful Parameterization of the multi-layered ANNs' feed-forward technique with standard back-propagation algorithm is the key element of the analysis. However, the ANNs procedures were performed by using the trial and error approach. Even though this approach was used, it was directed by the researcher based on learning the basic concept of setting the parameters of the analysis that was mentioned above. Therefore, a set of chosen internal parameters was specified and fixed in the three-date imagery of the study area (Table 2). The number of iteration was set at the value of 500 after several trials were experimented. Even though the Iter.No was set to a user-defined- value, the training process would stop when the maximum number of iteration was reached. Three-date classified images were produced (Figure 6) as well as three more ANNs resultant RMS_E scatter plots. A rule image classifier subroutine in ENVI® was used to produce binary image for each class individually in each year.

Table 2. The fixed parameterization of the multi-layered supervised ANNs' feed-forward technique with standard back-propagation algorithm.

Parameters of ANNs-supervised classifier*	AF	T-Th	TR	MO	T-RMS_E	HL	Iter.No
Selected Values**	Log.	0.9	0.2	0.9	0.1	1	500

* Abbreviations of parameters of ANNs supervised classifier : AF = activation function, T-Th = training threshold contribution, TR = training rate, MO = training momentum, T-RMS_E = training root mean square errors, HL = hidden layers, and Iter.No = number of training iterations.

** Abbreviations of selected values of AF : Log. = the logistic (sigmoid) activation function

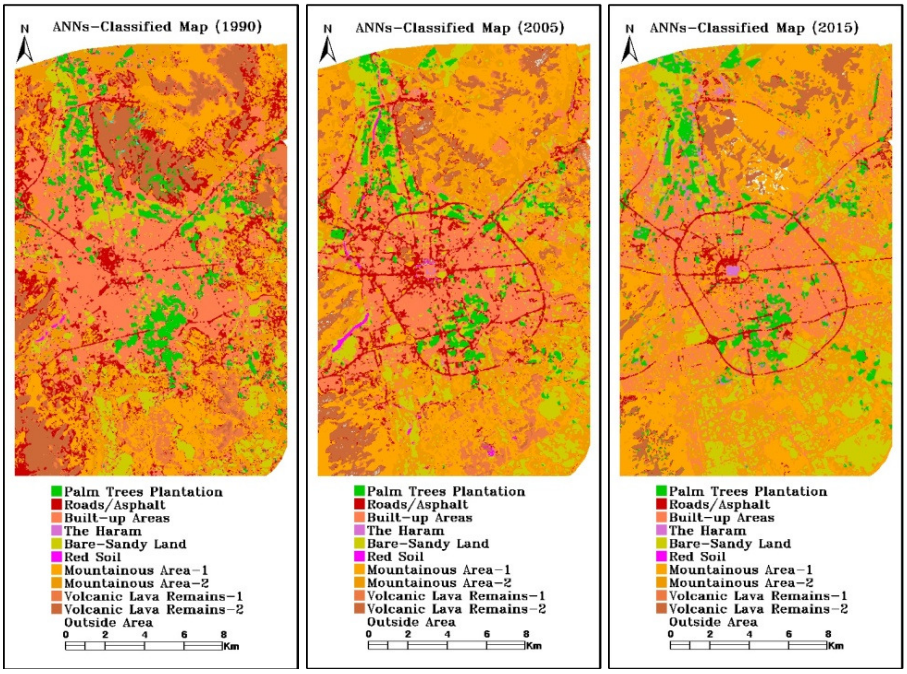

Figure 6. Subsets of three-date ANNs Classified Maps.

4-5 Post-Classification Preparation and Procedures

Training sites were regenerated and re-processed by merging all classes except the palm trees plantation and the outside area classes. Three classes only were generated in each date. These classes are: Planted Areas, Not-Planted areas, and Outside Area. Same ANNs classification analysis - that was developed to produce the mentioned above land cover classes - was used. Although there are only three classes in the classification process, the training sample is large in size. Same parameterization was followed in the procedure expect for the hidden layer (HL) parameter that was set to three instead of one. Three gray scale classified images (1990, 2005, and 2015) were developed as "planted/not-planted areas" maps to support the classification accuracy assessment of the binary palm trees plantation difference map in a later step (Figure 7).

Furthermore, a masking process was developed from the resultant (Planted/Not-Planted) classified images to create a binary image - the class in question in white (DN=1), all others masked out (DN=0) - for the palm trees plantation class in each year (Figure 8). Build Mask subroutine of ENVI® was used to perform the masking process. A palm trees plantation difference - (growth or decline) or in another word (gain or loss) - map was generated to visualize and quantify the difference in two periods (1990-2005 & 2005-2015) by using the resultant masked binary images.

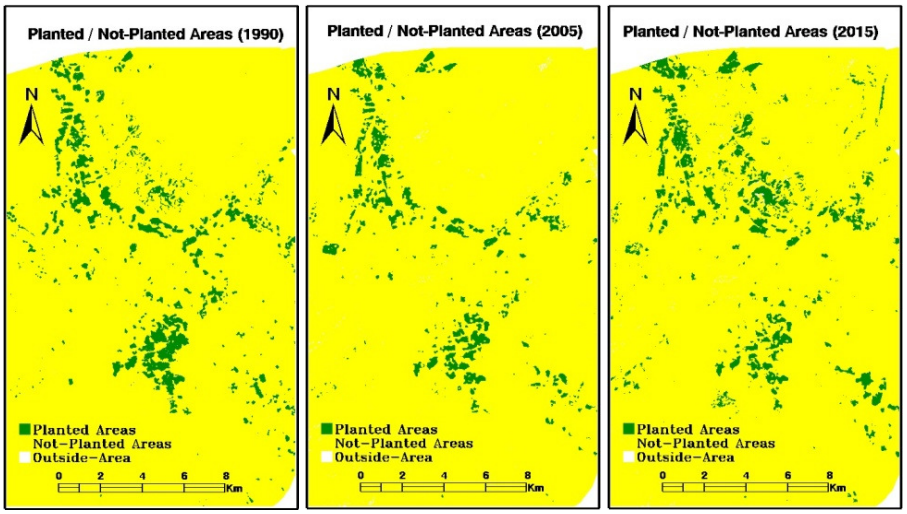

Figure 7. Subsets of "Planted / Not-Planted Areas" Classified Maps.

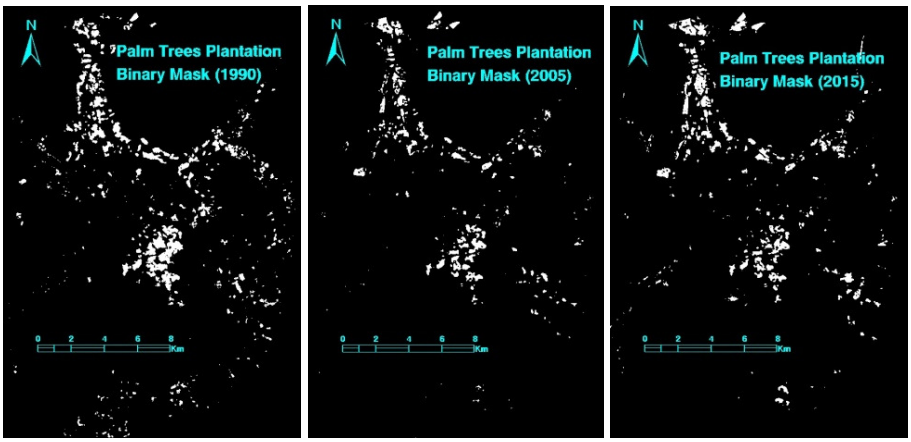

Figure 8. Subsets of three-date binary Maps of the palm trees plantation.

4-6 Change Detection Procedures

In this research, a post-classification comparison change detection algorithm was adopted to identify, discriminate, describe, and quantify differences and changes between images of study area at the three different dates of study (Shoukry, 2004). Two "change detection statistical matrix" reports were produced for the period of 1990-2005 and 2005-2015, respectively. Absolute area changing from a class in initial state image to another or same class in final state image was calculated, as well as the percentage of change. Since we are only concerned with palm trees plantation decline or growth versus urban sprawl in one hand and land reclamation & re- plantation on the other hand, four classes were excluded from analyzing the change detection matrix. These classes are roads/asphalt, the Haram, volcanic lava remains-1, and volcanic lava remains-2. The matrix indicates how initial state pixels were classified in the final state "from-to" information. It analyses class movements, shifting distribution (the change movement of each class in initial state image towards other classes in final state) during the change detection period, as well as the "no-change" status of each class itself (Shoukry, 2004).

5) Results and Discussions

Cautiously, analysts must pay attention when processing and analyzing multi-source, multi-spectral and multi-temporal remote sensing data. When dealing carefully with such data, significant results could be accomplished. This research has four main results. The first is the resultant three-date classified images accompanied with RMS_E scatter plots for each analysis. The second is the accomplished change detection statistical matrix reports for the two periods of study, while the third is the produced two periods' change detection difference maps based on the previously generated binary

masks. Lastly, accuracy assessments were achieved to quantitatively ensure and verify the proposed method.

5-1 Proposed ANNs Classification Internal Accuracy

When applying the ANNs classification, the system immediately generates a scatter plot to show the training processing. A systemically self-computed RMS_E of each iteration - based on the previously specified parameters by the researcher - was displayed in the plot. It should be noted that the RMS_E value should be decreased as the iteration number increases, but the system could act differently depending on the inputted parameters. Therefore, it is advisable to apply several trials before confirming the settled parameterization process. In this study, the researcher designed an identical set of parameters that was applied for each of the three-date image as it was mentioned above. Three scatter plots were produced specifying the value of RMS_E of each classified image. It shows significant results for the classified image of the year 1990, 2005, and 2015. The errors were 0.18, 0.11, and 0.27, respectively (Figures 9, 10, and 11).

5-2 Change Detection Statistical Matrix Reports

It is essential for the analyst to have a better understanding of class change from one date to another explaining the reason behind this change. Two change detection statistical matrix reports were generated for the two periods of study. The initial (former) state selected classes are listed in the columns of the matrix, while the final (later) state classes are listed in the rows. For each initial state class, the table indicates how these pixels were classified in the final state image. The measurements that were displayed in the matrix in square kilometers and percentages were identified. Table (3) represents the change between the year of 1990 and 2005. In the year of 1990, the total area of the "palm trees plantation" class was computed as 20.4 Km^2. It was noted that the area of the same class declined tragically in the year of 2005 to 13.7 Km^2 with a loss of 6.7 Km^2 of land area. Which means that the date palm trees planted land lost about 33% of its area in a period of 15 years apart. In one hand this is considered as a "loss" of date palm trees planted areas, while on the other hand is considered as a "gain" of other classes. On the expense of the palm trees planted area, the built- up class gained an area of 3.9 Km^2 representing itself about 58.2% of the total loss area. Another "gain" was oriented towards the bare-sandy land class. It gained an area of 2.1 Km^2, representing a percentage of 31.3% of the total loss area. This class represents a "man-made desertification" for the purpose of 'building preparation". These vacant lands were being prepared to be constructed by burning date palm trees and removing the soil in order to build on it (Figures 12 & 13). An area of 0.7 Km^2, representing a percentage of 10.5% of the total loss area, was oriented to other classes on the expanse of the class in question.

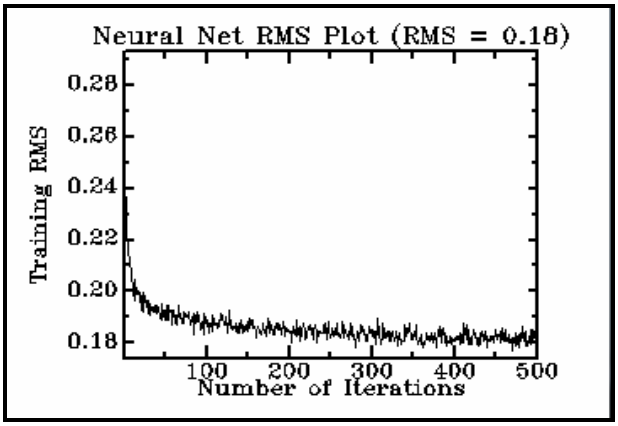

Figure 9. ANNs-RMS_E scatter plot of the 1990 classified image.

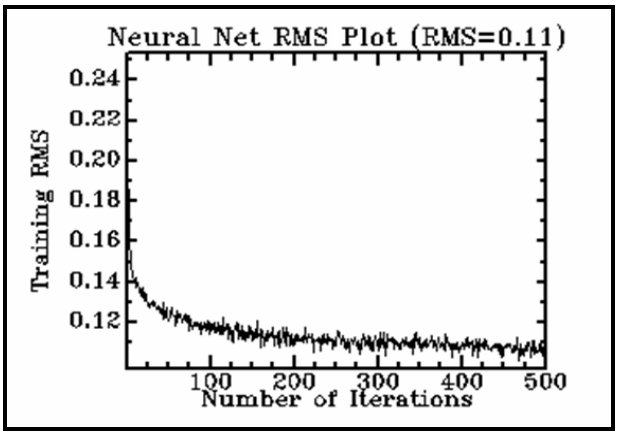

Figure 10. ANNs-RMS_E scatter plot of the 2005 classified image.

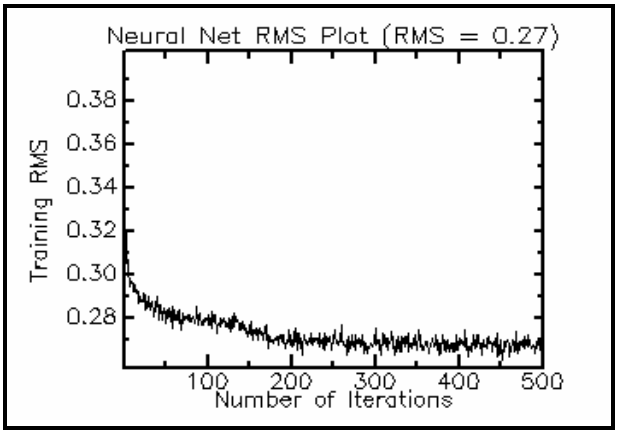

Figure 11. ANNs-RMS_E scatter plot of the 2015 classified image.

Table 3

Figure 12. Field photo (March-2014): A "man-made" desertification of date palm trees planted areas.

Figure 13. Field photo (March-2014): Burning date palm trees and removing the fertile soil.

Table (4) statistically measured the classes' change detection in the period of (2005-2015). In 2015, the total area of the "palm trees plantation" class was compensated and grew to reach 21.1 Km^2 with a gain of (+7.4 Km^2) of land area. The reason behind this positive change (gain) was due to the governmental awareness of the existence of this vital problem, which is the loss of palm trees to the urban sprawl. Therefore, the land reclaiming and re-planting policy was adopted by the government. Lands and low profitable loans were offered to the Saudi citizens in a trial of compensating the loss of palm trees planted areas. These lands were located mainly in the northern part far from the city core. Furthermore, the government established some public parks that were planted with palm trees within the city.

5-3 Change Detection Difference maps of Binary Masks

Two change detection difference maps (Figures 14 & 15) were generated based on processing the previously developed binary masks. The difference maps were produced from the resultant single-band (mono-band) gray scale images that have four classes each. The first class is "the unclassified pixels" that was a system self-generated class. This study succeeded to have zero unclassified pixels when it applied the analysis and computed the accuracy. The other classes were numerically specified to three by the researcher. Two types of changes were displayed in two classes. One represents the "gained" pixels, while the other represents the "lost pixels" during the two time periods of the class in question. The third class represents the "no-change" status. The generated difference maps succeeded to visually interpret the types of change as well as the change's trends in Al-Madinah Al-Munawarah study are a temporally.

5-4 The Research Accuracy Assessments Results

The research produced two accuracy assessment results. The first is developed for the resultant land cover classified images of the proposed ANNs classification method. The purpose of assessing the generated classification method's accuracy is to quantitatively evaluate its correctness, reliability, and significance that would affect the change detection analysis in a later step. The second is developed to evaluate the accuracy between the resultant binary masked images as assigned data and the (Planted/Not-planted) resultant classified images with its ground truth training sites as reference data. It should be noted that reducing the errors significantly would generate accurate change detection statistical matrix reports as well as producing highly accurate change detection difference maps of the study area.

Table 4

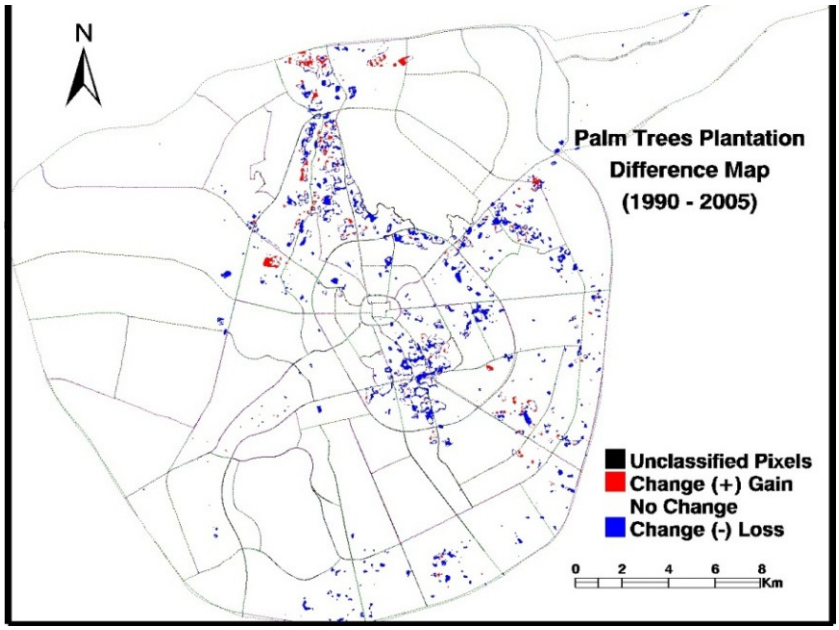

Figure 14. Change Detection Difference Map of the palm trees plantation in Al-Madinah Al-Munawarah (1990-2005).

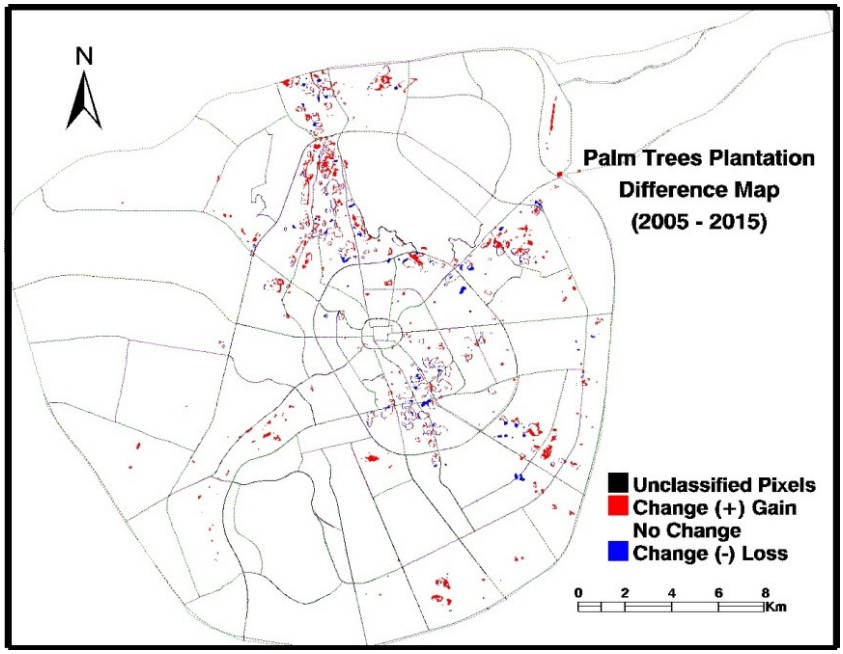

Figure 15. Change Detection Difference Map of the palm trees plantation in Al-Madinah Al-Munawarah (2005-2015).

The error matrix is a very effective way to represent accuracy because the accuracy of each category is clearly described (Jensen, 2005). The summary of the combined results of the accuracy assessment confusion (error) matrix report of the ANNs resultant land cover classified images was represented in Table (5). A sample set representing 10% of total ground truth training sites was stratified randomly generated for accuracy assessment of each date classified image. In 1990, a total sample set of 643 pixels - representing 10% of the total pixel size of the five previously chosen land cover classes for change detection analysis - was generated. A highly overall accuracy (OA) of 98.13% and a Kappa coefficient (*K*) of 0.98 were computed, indicating that all pixels were included in the assessment and unchanged pixels covered almost all study area. The assessment indicates that the unclassified pixels have a zero value. Commission (inclusion) errors (CE) as well as consumer (user) accuracies (CA) - that actually correspond to their classes on the ground - were both calculated for each class. The "palm trees plantation" class has reached a 100% consumer accuracy with zero value of commission errors. Moreover, omission (exclusion) errors (OE) as well as producer accuracies (PA) obtained a value of zero and 100% for the class in question, respectively. The 2005 accuracy assessment calculated the highest OA of the three-date classified images with a percentage of 99.5 and *K*=0.99. The total sample size was 632 pixels. Both CA and PA have a percentage of 100 with no errors of commission and omission. As for the 2015, the sample size was 565 pixels with OA=97.9 and *K*=0.97. The PA have a percentage of 100 with zero OE, while the CA have a percentage of 99.3 with 0.7 CE for the class in question.

Table (6) represents the accuracy assessment of the three-date "Planted/Not-planted" binary masks. A stratified randomly sample set - representing 10% of total ground truth training sites of the "Planted/Not-planted" classified image - was generated. In 1990, a total sample size of 1022 pixels was systemically selected. The overall accuracy (OA) reached 99.8% with a kappa coefficient (*K*) of 0.99. The total sample size of the year 2005 was 969 pixels with an (OA=98.9) and a (*K*=0.96), while the total sample size of the year 2015 was 881 pixels with same resultant overall accuracy and Kappa coefficient as 2005.

Table 5

Table 6

6) Conclusions and Recommendations

This research contributes to the field of remote sensing science' studies from conceptual, technological, and application perspectives. At the conceptual level, the present study has produced the rightful concepts of all the examined above analyses. Moreover, it would conceptually correct some misleading studies especially in the area of change detection. This study conceptually started with analyses such as MSCF & NDVI and ended with ANNs land cover classification & change detection.

Technologically, this research has developed and generated a new method in the field of remotely sensed ANNs analysis. The merging of filtering analysis of MSCF and the infusion of the transformation analysis of NDVI, with the adopted ANNs algorithm and its parameterization settings that was designed by the researcher, has offered a promising highly accurate new method that would be used effectively to enhance change detection analyses. Moreover, the selection of the appropriate change detection algorithms with the preservation of the analyses' terms and conditions is a corner stone in the analysis.

At the application level, this study has established a well documented micro-scale application. The application was specified on studying the date palm trees plantation in Al-Madinah Al-Munawarah for a period of 25 years (1990-2015). Therefore, It is recommended to expand the use of advanced artificial intelligence techniques in the field of remote sensing by using different data source and different case studies. For future researches, it is recommended to adopt and experiment advanced remotely sensed change detection methods such as 3D change detection.

REFERENCES

1. Ahmadizadeh, S., Yousefi, M., and Saghafi, M., 2014, Landuse change detection using remote sensing and artificial neural network: Application to Birjand, Iran. *Computational Ecology and Software*, 4(4):276-288.
2. Ashish, D., McClendon, R.W., and Hoogenboom, G., 2009, Land-use classification of multispectral aerial images using artificial neural networks. *International Journal of Remote Sensing*, 30(8):1989-2004.
3. Berberoglu, S., Lioyd, C.D., Atkinson, P.M., and Curran, P.J., 2000, The integration of spectral and textural information using neural networks for land cover mapping in the Mediterranean. *Computers and Geosciences*, 26(4):385-396.
4. Campbell, J.B., 1996, Introduction to remote sensing, 2nd ed., NewYork: The Guilford press.
5. Dai, X. L. & Khorram, S., 1999, Remotely sensed change detection based on artificial neural networks. *Photogrammetric Engineering and Remote Sensing*, 65(10):1187-1194.

6. Deilmai, B.R., Kanniah, K.D., Rasib, A.W., and Ariffin, A., 2014, Comparison of pixel-based and artificial neural networks classification methods for detecting forest cover changes in Malaysia. *8th International Symposium of the Digital Earth (ISDE8), IOP Conf.Series: Earth and Environment Science*, 18:1-5.
7. Del Frate, F., Pacifici, F., Schiavon, G., and Solimini, C., 2007, Use of neural networks for automatic classification from high-resolution images. IEEE Transactions on Geoscience and Remote Sensing, 45(4):800-809.
8. Deren Li, 2010, Remotely sensed images and GIS data fusion for automatic change detection. *International Journal of Image and Data Fusion*, 1(1):99-108.
9. Fitzgerald, R.W. & Lees, B.G., 1996, Temporal context in floristic classification. *Computers and Geosciences*, 22(9):981-994.
10. Foody, G.M., 1997, Fully fuzzy supervised classification of land cover from remotely sensed imagery with an artificial neural network. *Neural Computing & Applications*, 5(4):238-247.
11. Foody, G.M., Lucas, R.M., Curran, P.J., and Honzak, M., 1997. Non-linear mixture modelling without end-members using an artificial neural network. *International Journal of Remote Sensing*, 18(4):937-953.
12. GDMS, 2001, Print out map of merged IRIS-Landsat satellite images of Al-Madinah Al-Munawwarah (map scale 1:50,000), General Directorate of Military Survey, Ministry of Defense and Aviation, Kingdom of Saudi Arabia (K.S.A).
13. GDMS, 2001, Al-Madinah Al-Munawwarah Topographic Map (scale 1:50,000), General Directorate of Military Survey, Ministry of Defense and Aviation, Kingdom of Saudi Arabia (K.S.A).
14. Gopal, S. & Woodcock, C.E., 1996, Remote sensing of forest change using artificial neural networks. *IEEE Transactions on Geoscience and Remote Sensing*, 34(2):398-404.
15. Gopal, S. & Woodcock, C.E., 1999, Artificial neural networks for detecting forest change. In: C. H. Chen (ed). *Information processing for remote sensing*, Singapore: World Scientific Publishing Co., pp. 225-236.
16. Jensen, J.R., 2005, Introductory digital image processing: A remote sensing perspective, 3rd ed., Englewood cliffs. NJ: Prentice Hall Inc.
17. Ji, C.Y., 2000, Land-use classification of remotely sensed data using kohonen self-organizing feature map neural networks. *Photogrammetric Engineering and Remote Sensing*, 66(12):1451-1460.
18. Keiner, L.E., 1999, Neural Networks as non-linear function approximators for remote sensing applications. In, Chen, C.H., (ed.) *Information Processing for Remote Sensing*, U.S.A:World Scientific Publishing Co. Pte. Ltd.
19. Lillesand, T.M. & Keifer, R.W., 2000, Remote sensing and image interpretation, 4th ed., New York: John Wiley and Sons, Inc.
20. Liu, X. & Lathrop, R. G. JR, 2002, Urban change detection based on an artificial neural network. *International Journal of Remote Sensing*, 23(12):2513-2518.
21. Lu, D., Mausel, P., Brondizio, E., and Moran, E., 2004, Change Detection Techniques. *International Journal of Remote Sensing*, 25(12):2365-2407.

22. Mann, S. & Benwell, G.L., 1996, The integration of ecological, neural and spatial modelling for monitoring and prediction for semi-arid landscapes. *Computers and Geosciences*, 22(9):1003-1012.
23. Mannan, B., Roy, J., and Ray A.K., 1998, Fuzzy ARTMAP supervised classification of multi-spectral remotely-sensed images. *International Journal of Remote Sensing*, 19(4):767-774.
24. Matsah, M.I. & Hossain, D., 1993, Ground conditions in Al-Madinah Al-Munawarah, Saudi Arabia, *JKAU: Earth science*, 6, pp.47-77.
25. McCulloch, W.S. & Pitts, W., 1943, A logical Calculus of the ideas immanent in nervous activity. *Bulletin of Mathematical Biophysics*, 5, pp.115-133 (reprinted in the *Bulletin of Mathematical Biology*, 52(1/2):99-115 in 1990).
26. Minsky, M.L. & Papert, A., 1969, Perceptron: An Introduction to Computional Geometry, Expanded Edition. Cambridge, MA: MIT Press, 1988.
27. Mokhtarzade, M., Valadan Zoej, M.J., and Ebadi, H., 2008, Automatic road extraction from high resolution satellite images using neural networks, texture analysis, fuzzy clustering and genetic algorithms. *The International Archives of the Photogrammetry, Remote Sensing and Spatial Information Sciences*, Beijing, XXXVII(B3b):549-555.
28. Ojaghi, S., Ebadi, H., and Ahmadi, F.F., 2015, Using artificial neural network for classification of high resolution remotely sensed images and assessment of its performance compared with statistical methods. American Journal of Engineering, Technology and Society, 2(1):1-8.
29. Peterson, C. and SÖderberg, B., 1993, Artificial neural networks. In, Reeves, C. (ed.) *Modern Heuristic Techniques for combinatorial Problems*, New York: John Wiley.
30. Petropoulos, G.P., Vadrevu, K.P., Xanthopoulos, G., Karantounias, G., and Scholze, M., 2010, A comparison of spectral angle mapper and artificial neural network classifiers combined with landsat TM imagery analysis for obtaining burnt area mapping. *Sensors*, 10(3):1967-1985.
31. Rosenblatt, F., 1958, The Perceptron: a probabilistic model for information storage and organization in the brain. *Psychological Review*, 65:386-408.
32. Rouse, J.W., Haas, R.H., Schell, J.A., and Deering, D.W., 1974, Monitoring vegetation systems in the great plains with ERTS. *Proceedings, 3rd ERTS Symposium*, 1:309-317.
33. Serpico, S.B., Bruzzone, L., and Roli, F., 1996, An experimental comparison of neural and statistical non-parametric algorithms for supervised classification of remote sensing images. *Pattern Recognition Letters*, 17(13):1331-1341.
34. Seto, K.C. & Liu, W. G., 2003, Comparing ARTMAP neural network with the maximum likelihood classifier for detecting urban change. *Photogrammetric Engineering and Remote Sensing*, 69(9):981-990.
35. Shoukry, N.A., 2004, Using Remote Sensing and Geographical Information Systems for Monitoring Settlement Growth Expansion in the Eastern Part of the Nile Delta Governorates in Egypt (1975-1998), Ph.D. Dissertation, Department of Geography, The University of Utah: Salt Lake City, U.S.A.
36. Zhang, J. & Foody, G.M., 2001, Fully-fuzzy supervised classification of sub-urban land cover from remotely sensed imagery: statistical and artificial neural network approaches. *International Journal of Remote Sensing*, 22(4):615-628.

37. Zhang, Z., Verbeke, L., De Clercq, E., Ou, X., and De Wulf, R., 2007, Vegetation change detection using artificial neural networks with ancillary data in Xishuangbanna, Yunnan Province, China. *Chinese Science Bulletin*, 52(2):232-243.
38. Zhou, L., & Yang, X., 2008, Use of Neural Networks for land cover classification from remotely sensed imagery. The International Archives of the Photogrammetry, Remote Sensing, and Spatial Information Sciences, XXXVII(B7):575-578.